IEEE Access
Multidisciplinary | Rapid Review | Open Access Journal

Received March 11, 2019, accepted March 26, 2019, date of publication March 28, 2019, date of current version April 13, 2019.

Digital Object Identifier 10.1109/ACCESS.2019.2908028

Distributed Conflict-Detection and Resolution Algorithms for Multiple UAVs Based on Key-Node Selection and Strategy Coordination

YU WAN, JUN TANG, AND SONGYANG LAO
College of Systems Engineering, National University of Defense Technology, Changsha 410073, China
Corresponding author: Jun Tang (jun.tang@e-campus.uab.cat)

ABSTRACT A distributed conflict-detection (CD) and resolution algorithm for multiple unmanned aerial vehicles based on key-node selection and strategy coordination are proposed in this paper. Each aircraft is regarded as a critical node in a complex network. A novel temporal and spatial integrated CD methodology is proposed for aircraft formations and clusters. Each node selects three candidate strategies from a pre-set pool of strategies and generates corresponding planned tracks using uncertainty modeling based on the 6 degrees-of-freedom motion. The primary combination of strategies required for coordination of the aircraft in conflict is based on the maximum-robustness principle. To address partial knowledge of the environment, a special token-allocation strategy for coordination with incomplete information is proposed in this paper. To address potential data dropouts, this study damps the solution to achieve coordination. Two extreme scenarios are constructed to examine the proposed methodology. The results showed great collision-avoidance ability in continuous conflicts with multiple aircraft in a highly dynamic 3-D environment.

INDEX TERMS Collision avoidance, conflict-detection and resolution, distributed algorithm, strategy coordination, unmanned aerial vehicle, path planning.

I. INTRODUCTION

As technology develops, an increasing number of aircraft are pouring into the sky. Clustering, autonomy, intelligence have become the developing trends for unmanned aerial vehicles (UAVs). Conflict-detection and resolution (CDR) is the key to guaranteeing a normal aircraft flight. Most CDR algorithms are centralized; i.e., they assume a centralized point has a global perspective and determines optimal maneuvers for the current situation. However, centralized CDR algorithm have a single point of failure and restricted range [1]. Decentralized CDR algorithms can ensure flexibility and stability while dealing with a dynamic environment and address the UAV's tendency toward autonomy and clustering [2]. However, current decentralized algorithms mostly concentrate on solving pair conflicts and cannot satisfactorily manage multiple-aircraft conflicts.

To address this problem, this paper presents a novel distributed CDR algorithm for multiple UAVs, based on key-node selection and strategy coordination. An aircraft in conflict is regarded as a critical node in a complex network. A novel temporal-and-spatial-integrated (TASI) conflict-detection (CD) methodology, which integrates the spatial and temporal dimensions, is proposed for judging whether a conflict exists, further evaluating the risk degree between nodes, and determining the critical nodes. Each node chooses candidate strategies from a pre-set pool of strategies and generates corresponding plan tracks using uncertainty modeling based on six-degrees-of-freedom motion. Through coordinating the planned tracks, the aircraft determines an optimal strategy based on maximum robustness. To overcome the uncertainty of the track prediction, this paper introduces uncertainty model that replace a simple trajectory with a cone that combines the future position and error radius; To overcome partial knowledge, a special token-allocation method is used; To overcome a potential data dropout, this paper introduces damping into the solution to achieve coordination.

The associate editor coordinating the review of this manuscript and approving it for publication was Rashid Mehmood.

TABLE 1. Summary of publication addressing the CDR problem.

Publication	Dimension	Communication (Cooperative/ Non-cooperative)	Number		Resolution		Global	
			Pair	Multiple	Tactical	Strategic	Centralized	Decentralized
[4]	3D	Cooperative	√		√		√	
[6]	3D	Cooperative	√		√		√	
[7]	3D	Cooperative	√		√		√	
[8]	3D	Non-cooperative	√		√		√	
[5]	3D	Cooperative	√		√		√	
[9]	3D	Cooperative		√	√			√
[11]	3D	Cooperative		√		√		√
[12]	3D	Non-cooperative	√			√	√	
[13]	3D	Cooperative	√			√	√	
[15]	3D	Cooperative		√		√		√
[19-21]	3D	Cooperative	√					√
[23-25]	3D	Cooperative		√				√

This study further ensures scalability and flexibility and improves the overall performance by increasing the robustness to information inconsistencies.

This paper is organized as follows: Section 2 summarizes current CDR algorithms; Section 3 describes algorithm model. Specially, part A describes the TASI CD model; part B presents a track-management model based on six-degrees-of-freedom motion; part C presents a strategy-generation model based on maximum robustness; part D presents the decentralized-coordination model based on a special token-allocation method and part E presents the primary-activation module, based on noninterference principle; Section 4 presents the simulation experiments; Finally, the conclusion and future works are summarized in Section 5.

II. LITERATURE REVIEW

The various CDR methods for aircraft can be sorted into two general types: i.e., tactical and strategic [3]. Tactical CDR methods include geometric algorithms (GA), which implement passive collision avoidance (CA) through analyzing the geometric relationships between aircraft. Strategic CDR methods include trajectory-planning algorithms, which plan a collision-free flight path from the current position to a target position under minimum security constraints. A detailed summary of publications is provided in Table 1.

The point of closed approach (PCA) and the collision cone approach (CCA) are two typical geometric algorithms. PCA calculates the time τ to the closed approach point and the miss distance vector r_m to detect a collision. Park *et al.* [4] propose 'Vector Sharing Resolution' maneuvering logic to solve the conflict. Han *et al.* [5] improve PCA by introducing a navigation coefficient to balance the optimality and security of the CA strategy. The basic principle of CCA is to create a sphere centered at the invader aircraft, the tangent lines from the current aircraft to the sphere constitute a collision cone. The optimal CA strategy is generated by adjusting the current aircraft's relative velocity to be tangent to the sphere [6]. Carbone *et al.* [7] and Luongo *et al.* [8] improve CCA by building a cylindrical safety bubble to consider different minimum separation on the vertical and horizontal planes. Smith and Harmon [9] develop an aggregated collision-cone approach to allow each UAV to simultaneously detect and avoid collisions with more than two aircraft. Geometric algorithms are simple and intuitive; however, most focus on pairwise encounters, for its calculation amount is inconsiderably massive for multiple aircraft [10].

Trajectory-planning algorithms include the artificial potential field (APF) algorithm, linear programming, the A$*$ grid-based algorithm, etc. Sigurd and How [11] investigate the feasibility of a total field-sensing approach to avoid collisions through the collective navigation of multiple aircraft in constrained spaces. Liu *et al.* [12] combine the Lyapunov method with APF to help the UAV escape the saddle point when avoiding a collision. Temizer *et al.* [13] formulate the CA problem as a partially observable Markov decision process (POMDP) and proposes a generic POMDP solver to generate avoidance strategies. The A$*$ grid-based algorithm, based on Dijkstra's algorithm, works by traversing a graph to plan the shortest safe flight path between nodes [14]. Alliot *et al.* [15] propose a coordinated and decentralized embarked conflict solver based on the A$*$ algorithm, by continuously combining simple maneuvers. Richards and How [16] propose a mixed-integer linear programming (MILP) solver that takes the constraints and attempts to find the optimal path by manipulating the force affecting how much a single aircraft turns at each time step.

Van Den Berg *et al.* [17] present a formal approach to reciprocal n-body collision avoidance for multiple mobile robots by reducing the problem to solving a low-dimensional linear program. Holt *et al.* [18] compare the performance of APFs, MILPs, and dynamic sparse A$*$ search (DSAS) and concludes that APF has the highest overall performance, MILP is both effective and efficient with a small number of aircraft, DSAS is more effective when a larger airspace is available for maneuvering.

Other CA algorithms are available, in addition to the above CA algorithms for UAVs; e.g., the traffic collision avoidance

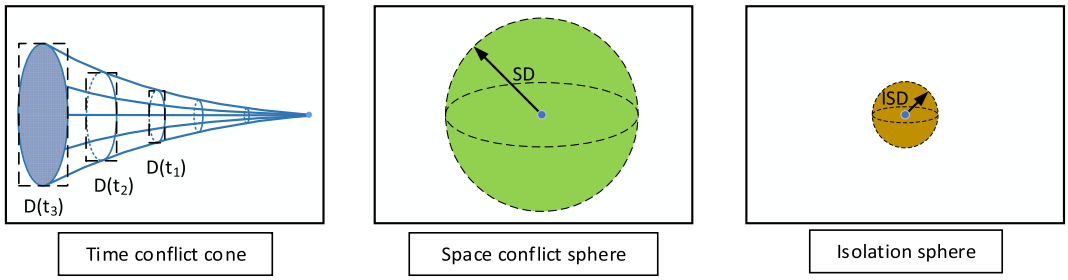

FIGURE 1. Temporal and spatial integrated and conflict detection zone.

system (TCAS) for civil aviation aircraft and the automatic aircraft collision avoidance (Auto-ACAS) for fighter aircraft. TCAS is designed as the final safeguard to resolve midair collisions and evidently decreases near midair collisions in global airspace [19]–[21]. TCAS only suggests resolution advisories (RAs) for the pilot when a collision could conceivably appear within 15 to 35s. The RA are only in the vertical direction (upward, downward). Despite its ability of to deal with multi-aircraft encounters, TCAS sometimes issues improper RAs in complex situations [22]. Auto-ACAS was developed for fighter aircraft operating in an air combat training environment [23]–[25]. Auto ACAS performs an automatic, aggressive strategy to avoid collisions with other aircraft. It coordinates and determines the combination of strategies that provides the best separation, and initiates strategies when a collision is imminent. And it provides good reference for this paper.

III. MODEL

In local airspace, unmanned aerial vehicles (UAVs) form a dynamic complex network in which nodes represent aircraft in conflict, and edges have attributes representing the risk degree. Each node selects three candidate strategies from the pre-set pool of strategies, according to the relative situation between the nodes. The track management unit generates three planned tracks corresponding to the three candidate strategies. According to the maximum-robustness principle, the nodes coordinate with each other to determine the optimal strategy that ensures the maximum network security. The nodes coordinate through a token-allocation method. When the UAVs are about to collide, i.e., when the planned tracks of aircraft intersect in space at a certain moment, aircraft will activate the optimal CA strategy. The entire UAV network is constantly being updated.

A. TEMPORAL-AND-SPATIAL-INTEGRATED CONFLICT-DETECTION UNIT

The function of the CD unit is to judge whether a conflict exists, based on the situation between the aircraft, evaluate the possibility of a collision, and calculate the risk degree between the nodes and critical nodes. When UAVs fly in formation, the distance between pairs is relatively small; however, if their approaching speed is very small and their flight plans do not overlap, there is no collision risk between them. The traditional CD algorithm based on spatial distance has several limitations and can lead to false alarm in aircraft formations and clusters.

In this study, a novel TASI CD model was constructed, which integrates the spatial and temporal dimensions for CD. For two aircraft to be conflict, they need to satisfy both the time and space conflict conditions simultaneously. As shown in Figure 1, the CD area has three overlapping parts: the space-conflict sphere, the time-conflict cone and the collision sphere.

The space-conflict sphere uses a sphere of radius SD (the safe distance) centered at the aircraft. The space-conflict sphere is based on the Euclidean distance; the judge condition is as follows:

$$\sqrt[2]{\left(x_i^{t_0}-x_j^{t_0}\right)^2+\left(y_i^{t_0}-y_j^{t_0}\right)^2+\left(z_i^{t_0}-z_j^{t_0}\right)^2}<SD \quad (1)$$

where $P_i^{t_0} = \left[x_i^{t_0}\ y_i^{t_0}\ z_i^{t_0}\right]$ is the position of aircraft i at moment t and $P_j^{t_0} = \left[x_j^{t_0}\ y_j^{t_0}\ z_j^{t_0}\right]$ is the position of aircraft j at moment t.

The time-conflict cone uses the current position as the starting point of the track, i.e., it represents possible aircraft position from current moment t_0 to future moment $t_0 + \mathrm{T}$. When two aircraft conflict in spatial dimension, their future-track cones will converge in time and space. The judge condition of time conflict cone is as follow:

$$\exists t \in (t_0, t_0+T)\left(D(t)^i - D(t)^j\right) < ISD \quad (2)$$

where $D(t)^i$ is a disk centered at the predicted position, which represents the possible positions of aircraft i at future moment t, considering possible errors. ISD is the isolation-sphere radius.

The isolation sphere is the safety separation zone for an aircraft. It is a sphere whose radius ISD is the sum of the wingspan and the desired separation distance (DSD). If an aircraft crosses into the isolation sphere of another aircraft, it is regarded as a collision.

Each aircraft is regarded as a node in a network, and aircraft in conflict are linked by a line with attribute R_{ij} representing the degree of conflict. The risk degree is related to relative the Euclidean distance RS_{ij} and the approaching speed RD_{ij}. If the UAVs are separating, RS is negative and eliminated from the equation. If the UAVs are approaching,

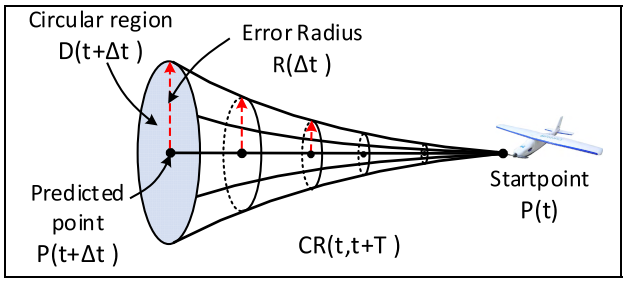

FIGURE 2. The planned track.

RS is positive. u, v and w are the speed state, x, y and z are position state.

$$R_{ij} = \frac{RS_{ij}}{RD_{ij}}, RS > 0 \tag{3}$$

$$RD_{ij} = \sqrt{(u_i - u_j)^2 + (v_i - v_j)^2 + (w_i - w_j)^2} \tag{4}$$

$$RS_{ij} = \frac{(x_i - x_j)\times(u_i - u_j) + (y_i - y_j)\times(v_i - v_j) + (z_i - z_j)\times(w_i - w_j)}{\sqrt{(x_i - x_j)^2 + (y_i - y_j)^2 + (z_i - z_j)^2}} \tag{5}$$

For each node, the criticality E is the sum of the risk degrees between the current aircraft and the intruder aircraft. $j \in \{1, 2, \ldots, N\}$ represents all aircraft in conflict with aircraft i. The larger an aircraft's criticality of aircraft is, the higher its priority is in cooperating.

$$E_i = \sum_{j=1}^{n} R_{ij}, \quad j \in \{1, 2, \ldots, N\} \tag{6}$$

B. TRACK-MANAGEMENT UNIT BASED ON SIX-DEGREES-OF-FREEDOM MOTION

In the algorithm, the track-management model manages the track of an aircraft, including its own track-management part and the intruder track-management part. Firstly, the former predicts its own future flight path for a period and generates the time-conflict cone for CD; secondly, it generates three planned tracks corresponding to the candidate strategies. The corresponding planned track is the future track if the aircraft takes the candidate strategy. In the track-prediction process, UAV state prediction poses some uncertainties, including: (1) navigation uncertainty; (2) trajectory prediction uncertainty; (3) trajectory reconstruction / fitting uncertainty; (4) data-link transmission uncertainty; and (5) trajectory-data calculation uncertainty. Therefore, this paper introduces an uncertainty model, which forms a cone combining the future position and error radius to ensure that all the actual future positions $Q(t + \Delta t)$ will fall into the region. As shown in Figure 2, we extend the predicted point at some moment to a disk D $(t + \Delta t)$ of radius R (Δt) centered at P $(t + \Delta t)$. The center of the disk is a predicted position P $(t + \Delta t)$ obtained by six-degrees-of-freedom motions. The radius is the error radius R (Δt), which is related to the uncertainty and increases over time Δt. The disks at different moments constitute the conical region CR(t, t + Δt).

$$D(t+\Delta t) = \{Q(t+\Delta t) \,|\, \|Q(t+\Delta t) - P(t+\Delta t)\| < R(\Delta t)\} \tag{7}$$

$$CR(t, t+T) = \{D(t+\Delta t) \,|\, \forall \Delta t \in [0\ T]\} \tag{8}$$

The error radius R (Δt) is the following quadratic function:

$$R(\Delta t) = a*(\Delta t)^2 + b*\Delta t \tag{9}$$

Indexes a and b are interrelated with many elements, e.g., the aircraft performance, data link and environment. The values of a and b are set to 0.425 and 1.19, considering the performance of UAVs provided by our team and the requirements of the experiment. The values are got by fitting a quadratic to the time history on the run.

The states of the aircraft are $(u, v, w, x_e, y_e, z_e, \phi, \theta, \psi, p, q, r)$, including the speed state (u, v, w),position state (x_e, y_e, z_e),attitude state $[\phi\ \theta\ \psi]$ and attitude change state (p, q, r). The track-management module is based on the six-degrees-of-freedom motion. The forces and moments are approximated according to the standard build-up method using dimensionless coefficients [26] (a shorthand notation is used to write the equations in which $S_\theta = \sin\theta, C_\psi = \cos\psi$,etc.).

Translational kinematics:

$$\begin{bmatrix} \dot{x}_e \\ \dot{y}_e \\ \dot{z}_e \end{bmatrix} = \begin{bmatrix} C_\theta C_\psi & S_\phi S_\theta C_\psi - C_\phi S_\psi & C_\phi S_\theta C_\psi - S_\phi S_\psi \\ C_\theta S_\psi & S_\phi S_\theta S_\psi + C_\phi C_\psi & C_\phi S_\theta S_\psi - S_\phi C_\psi \\ -S_\theta & S_\phi C_\theta & C_\phi C_\theta \end{bmatrix} \begin{bmatrix} u \\ v \\ w \end{bmatrix} \tag{10}$$

Translational dynamics:

$$\begin{bmatrix} \dot{u} \\ \dot{v} \\ \dot{w} \end{bmatrix} = \begin{bmatrix} 0 & r & -q \\ -r & 0 & p \\ q & -p & 0 \end{bmatrix} \begin{bmatrix} u \\ v \\ w \end{bmatrix} + \frac{1}{m} \begin{bmatrix} F_x \\ F_y \\ F_z \end{bmatrix} \tag{11}$$

Rotational kinematics:

$$\begin{bmatrix} \dot{\phi} \\ \dot{\theta} \\ \dot{\psi} \end{bmatrix} = \begin{bmatrix} 1 & S_\phi S_\theta / C_\theta & C_\phi S_\theta / C_\theta \\ 0 & C_\phi & -S_\phi \\ 0 & S_\phi / C_\theta & C_\phi / C_\theta \end{bmatrix} \begin{bmatrix} p \\ q \\ r \end{bmatrix} \tag{12}$$

Rotational dynamics:

$$\begin{bmatrix} \dot{p} \\ \dot{q} \\ \dot{r} \end{bmatrix} = \begin{bmatrix} I^p_{pq} pq + I^p_{pr} qr \\ I^q_{pq} p^2 + I^q_{rr} r^2 + I^q_{pr} pr \\ I^r_{pq} pq + I^r_{qr} qr \end{bmatrix} + \begin{bmatrix} g^p_l & 0 & g^p_n \\ 0 & g^q_m & 0 \\ g^r_l & 0 & g^r_n \end{bmatrix} \begin{bmatrix} L_m \\ M_m \\ N_m \end{bmatrix} \tag{13}$$

Indeed, $I^p_{pq} = I_{xz}\left(I_{yy} - I_{zz} - I_{xx}\right) D$, $I^q_{pq} = -\frac{I_{xz}}{I_{yy}}$, $I^r_{pq} = \left(I_{xx} I_{yy} - I^2_{xz} - I^2_{xx}\right)$D, $I^p_{qr} = \left(I^2_{zz} - I_{yy} I_{zz} + I^2_{xz}\right) D$, $I^q_{pr} = \frac{(I_{zz} - I_{xx})}{I_{yy}}$, $\mathrm{D} = \left(I^2_{xz} - I_{xx} I_{zz}\right)^{-1}$, $I^r_{qr} = -\frac{I^p_{pq}}{I_{yy}}$, $I^q_{rr} = -I^q_{pp}$, $g^p_l = -I_{zz} D$, $g^p_n = -I_{xz} D = g^r_l$, $g^q_m = \frac{1}{I_{yy}}$, $g^r_n = -I_{xx} D$

As the CA strategy is usually activated three to four seconds before the collision, the forecast duration needs to exceed four seconds. To comprehensively balance the computation load and system requirement, the forecast duration

is set to five seconds. The unit will generate the corresponding planned tracks for the next five seconds. Considering the prediction accuracy, computation efficiency, and the actual performance of the UAVs comprehensively provided by our team, the frequency is set to 10 Hz. At intervals of 0.1 s, the aircraft updates its states, and generates candidate strategies and the corresponding planned tracks. The predicted track consists of 50 discrete positions.

At each step, after generating the planned tracks, the aircraft will transmit them to the other aircraft in conflict via a data link. To reduce the amount of data, only five future points at 1 s, 2 s,3 s,4 s,5 s are transmitted. The aircraft's intruder track-management unit receives and processes the data of the planned tracks from the intruder aircraft. When processing, it adopts the quadratic curve-fitting method to reconstruct the predicted and planned trajectories of the intruder aircraft with the five points.

C. STRATEGY GENERATION BASED ON MAXIMUM ROBUSTNESS

In this paper, the optimal CA strategy for an aircraft is generated, based on the maximum robustness principle of complex networks. There are two steps in strategy-generation procedure. In the first step, for each node (UAV in the network), three candidate strategies are selected from a pre-set pool of strategies, according to the relative positions of neighboring nodes, and the corresponding planned tracks are broadcasted to neighboring aircraft. In second step, through coordination and evaluation, each node selects an optimal strategy from the three candidate strategies, based on the maximum-robustness principle. When all nodes in the network have determined their optimal collision-avoidance strategies, the aircraft will continue to fly normally, waiting for the activation of the CA maneuver before implementing the strategy. During this process, the entire network is dynamically updating at a regular interval.

Fixed-wing aircraft have great flexibility and mobility and can change their flight state quickly through rolling and climbing. In relevant studies [23]–[25], strategies were chosen from a pre-set group of categories. Setting the categories in advance can reduce the system budget, improve the calculation speed, and ensure a rapid response. The pre-set pool of strategies should satisfy the following requirements: 1. it should comprise maneuvers in all directions, including vertical and horizontal directions; 2. the strategy should not exceed the aircraft's limitation. Considering the aircraft's performance and characteristics, the following nine strategies are defined in this study: (1) Roll greatly to left; (2) Roll moderately to left; (3) Roll slightly to left; (4) Roll greatly to right; (5) Roll moderately to right; (6) Roll slightly to right; (7) climb with a 1g overload; (8) dive with a -1g overload; (9) Maintain the current track;

In the first step, the pre-selection of candidate strategies is based on the geometric situation between the own aircraft and the intruder aircraft, including those in frond or behind, above or below, or to the left or right side of the aircraft. Pre-selection also take geometric situation of formation into consideration. Aircraft in the same formation should avoid maneuvering in opposite directions. If one aircraft chooses to roll to right, the other should not choose to roll to left.

Robustness is the key to system survival under abnormal and dangerous conditions. The primary strategy-generation principle is to choose the combination of strategies that can delay the activation of the CA maneuver as much as possible, on the premise of safety. In the proposed method, the robustness is related to the predicted minimum range (PMR). The greater the PMR between the aircraft is, the safer the network, the later the activation moment, and the higher the network robustness are.

The robustness R(N) is defined as follows:

$$\mathrm{R}\,(N) = \frac{1}{2}\sum_{i=1}^{N}\sum_{j=1}^{N}\omega_{ij}\,(m,n) \tag{14}$$

$$\omega_{ij}\,(m,n) = \begin{cases} e^{AD_{mn}(t_0,t_0+T)^{ij}-PMR}, & PMR \geq RD \\ -\infty, & RD < PMR \end{cases} \tag{15}$$

$$\begin{aligned} &PMR_{mn}\,(t_0, t_0+T)^{ij} \\ &\quad = min\left(\left|P_m\,(t_0+t)^i - P_n\,(t_0+t)^j\right|\right. \\ &\qquad \left. - R_m\,(t)^i - R_n\,(t)^j\right)\mathrm{t}, \quad \in (0,T) \end{aligned} \tag{16}$$

N is the number of aircraft in the network. $P_m\,(t_0+t)^i$ is the predicted position at moment t_0+t when aircraft i makes maneuver n, $R\,(t)^i$ is the error radius at moment t_0+t when aircraft i makes maneuver n. RD is the radius of the isolation sphere.

In second step, for a pair of aircraft in conflict, there are $3\times3=9$ strategy combinations. For three aircraft in conflict, there are $3\times3\times3=27$ strategy combination. The optimal strategy, generated through cooperation, is as follows:

$$\mathrm{ACT}(M_i\,(m)\,,\ M_j\,(n)\,,\ldots\ldots,) = \mathrm{argmax}\,(R\,(N)) \tag{17}$$

where $M_i\,(m)$ means that aircraft i chose strategy m and $M_j\,(n)$ means that aircraft j chose strategy n.

D. DECENTRALIZED COORDINATION BASED ON A SPECIAL TOKEN-ALLOCATION METHOD

For decentralized approaches, each UAV obtains state information through global positioning (GPS) and other sensors, communicates with other UAVs through a data link, and independently determines its own optimal strategy. However, the aircraft do not have the same situational awareness, as they do not have the same detection zones and they conflict with different aircraft. The main problems of decentralized approaches are a partial knowledge of the environment, and coordination and decisions with incomplete information [15].

Figure 3 shows an example of centralized aircraft coordination. For three aircraft in conflict, the system with a global perspective considers 27 ($3\times3\times3=27$) strategy combinations and chooses strategies a, e, and i as the optimal

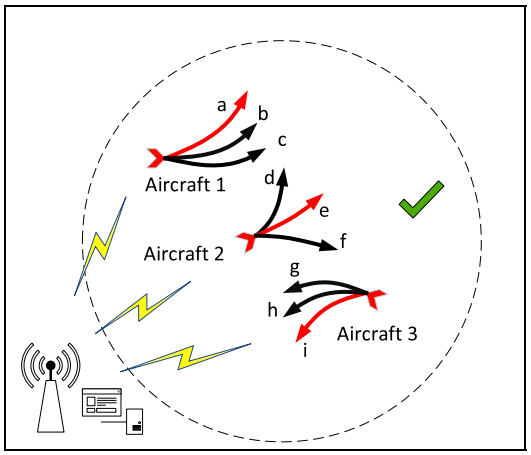

FIGURE 3. The centralized coordination.

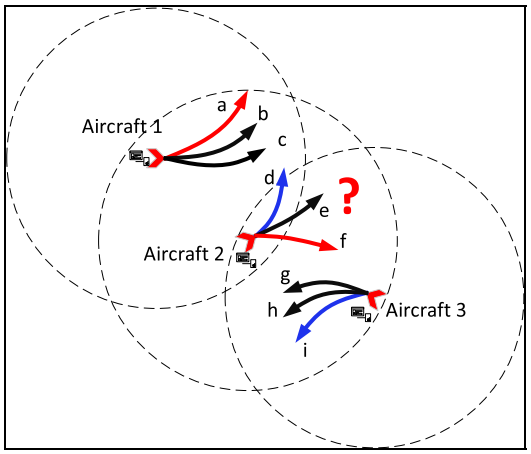

FIGURE 4. The decentralized coordination.

strategies for aircraft 1, 2, and 3, respectively. Figure 4 shows the decentralized aircraft coordination. Aircraft 1 and 2 are in conflict and aircraft 2 and 3 are in conflict, while aircraft 1 and 3 are not in conflict. For the aircraft 1 and 2 conflict, strategies a and f, respectively, are determined as the optimal ones. For the aircraft 2 and 3 conflict, strategies d and i are respectively determined as the optimal ones. For aircraft 2, the optimal strategies are inconsistent because it is in two different conflicts.

To improve the decentralized coordination, a special-token allocation method is formed [27]. Five steps are in the procedure, and we take a four-aircraft scenario as an example.

1. Calculate the risk degrees between pair nodes and criticalities of nodes in the network.

2. For two aircraft in conflict, the aircraft with a higher criticality delivers its own token and its received tokens to the one with a lower criticality.

3. In the entire network, the aircraft that did not receive tokens is regarded as key nodes. When coordination and evaluating, the key nodes first evaluate their three candidate strategies with other aircraft in conflict and determine the optimal strategy. Aircraft with one or more tokens are not considered.

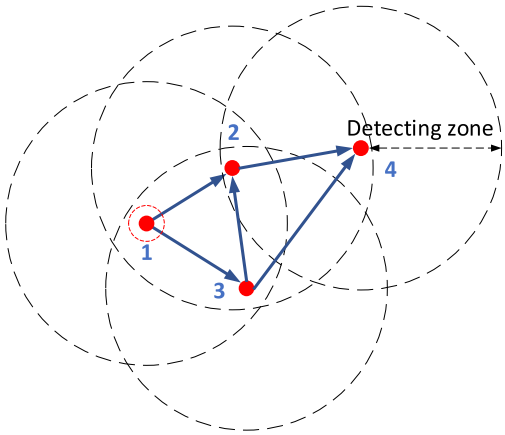

FIGURE 5. The centralized coordination.

4. Having determined the optimal strategy, the key nodes broadcast the strategy to the linked. All nodes that have received a token from this key node consider this optimal strategy, and then cancel the token received from the key node.

5. Steps 3 and 4 are repeated until no tokens remain.

As shown in Figure 5, aircraft 1 is in conflict with aircraft 2 and 3; aircraft 2 is in conflict with 4, and aircraft 3 is in conflict with 2 and 4. Aircraft 1 and 4 are not in conflict.

- Aircraft 1 passes its token to aircraft 2 and 3.
- Aircraft 3 passes its token and the token received from aircraft 1 to aircraft 2 and 4.
- Aircraft 2 passes its token and the tokens received from aircraft 1 and 3 to aircraft 4.

Figure 6 depicts the entire coordination and resolution process, and Table 2 records the token allocation at the different steps. Firstly, all aircraft broadcast their three planned tracks to the adjacent nodes. Then, in step 1, aircraft 1, with no token, coordinates with aircraft 2 and 3 to determine its optimal strategy. Then, it broadcasts its optimal strategy, and all aircraft that have received a token from it cancel the token. In step 2, aircraft 3, with no taken, coordinates with aircraft 2 and 4 while considering the optimal strategy of aircraft 1. Then, aircraft 3 broadcasts its optimal strategy, and all aircraft that have received a token from it cancel the token. In step 3, aircraft 2, with no taken, coordinates with aircraft 4, while considering the optimal strategies of 1 and 3. After determining its optimal strategy, aircraft 2 broadcasts it and aircraft 4 cancels the token from aircraft 2. In step 4, aircraft 4 considers the optimal strategies of aircraft 2 and 3 to determine its optimal strategy. (Aircraft 1 is not in the detection zone of aircraft 4, and thus, is not in conflict).

The aircraft state and network are highly dynamic. The aircraft-state update and the generation and sharing of the three planned tracks are at a frequency of 10 Hz. When generating the candidate strategies, the coordination and resolution of the optimal strategies are at a frequency of 4 Hz. The different frequency settings are due to the following consideration.

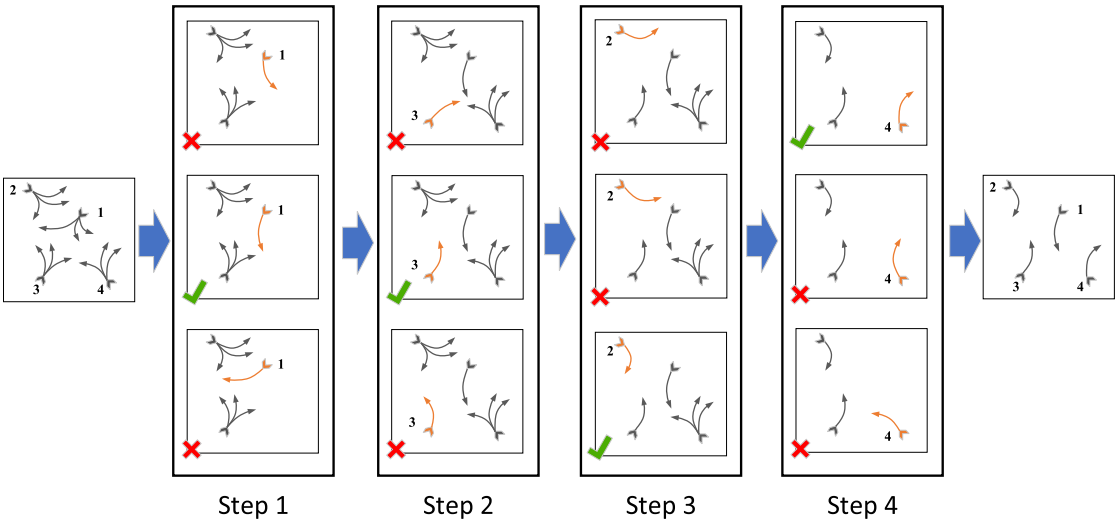

FIGURE 6. The procedure of coordination.

TABLE 2. Number of tokens in different steps.

Number of tokens	Step 1	Step 2	Step 3	Step 4
Aircraft 1	0*			
Aircraft 2	2	1	0*	
Aircraft 3	1	0*		
Aircraft 4	3	2	1	0*

In an actual situation, there are delays and the possibility of data dropouts when transmitting. If the two frequencies are set to be the same, the coordination may get out of phase and possibly result in uncoordinated maneuvers [24]. To solve this problem, this paper purposefully damps the solution to achieve coordination. Rather than choosing candidate strategies and determining the optimal combination at each update frequency, it happens periodically. During the other steps, the three candidate strategies do not change; however, the planned tracks are updated based on the updating states. Before the coordination, each aircraft will receive the planned tracks from other aircraft more than once. That will greatly increase the robust of the algorithm.

E. MANEUVER ACTIVATION BASED ON NONINTERFERENCE

The CA algorithm provides protection for aircraft in abnormal and dangerous conditions. Moreover, it should minimize the interference to the normal aircraft flight pattern on the premise of ensuring safety. Therefore, the principle of the proposed methodology is to activate CA strategies as late as possible.

As shown in Figure 7, aircraft A and B have a collision risk. Before aircraft A crosses the isolation sphere of aircraft B, it can take various strategies to avoid a collision. Due to aircraft-performance restriction, e.g., the minimum turning radius and, maximum turning angle, if they approach too close, i.e., exceed some moment (defined as the critical moment), aircraft A cannot avoid a collision with aircraft B,

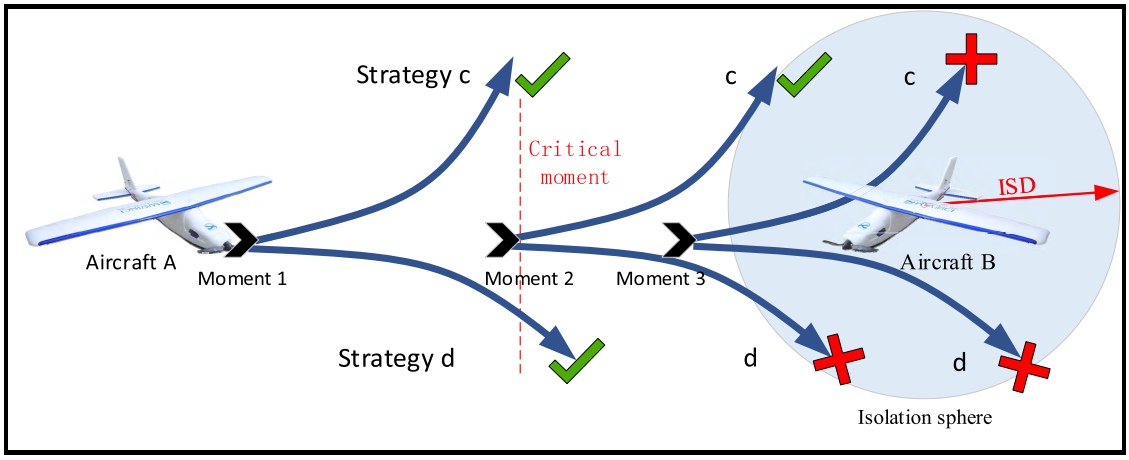

FIGURE 7. The principle of noninterference.

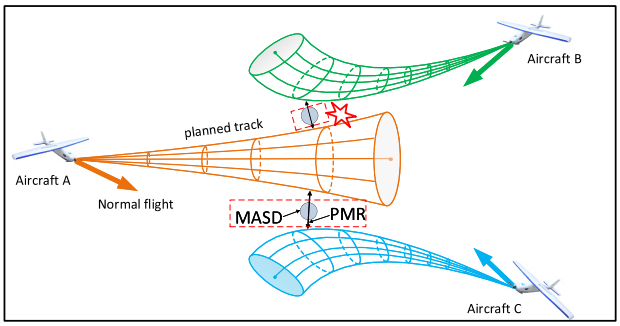

FIGURE 8. Activation of optimal strategies.

no matter what strategy it takes. The critical moment is the latest moment for two aircraft to avoid a collision; it is related to the performance, state, and relative placement.

Suppose c and d are the only strategies that the aircraft can take to avoid a collision. In Figure 7, at moment 1, aircraft A can choose strategy c or d to avoid a collision, however, it is too early and will greatly affect the normal flight pattern. At moment 3, a collision is unavoidable, regardless of the strategy. At moment 2, strategy c could avoid a collision, while d could not. Moment 2 is the last moment to avoid a collision and is the critical moment.

Thus, under the principle of noninterference, the critical point is the last moment, but also the best moment, for an aircraft to maneuver to avoid a collision. In the network, there is a critical activation moment between any two connected nodes. For multiple connected nodes, the CA strategy is triggered as soon as any critical point is reached. The pairs that activate CA strategies move along the predicted tracks, while the other aircraft continue their normal flight.

As shown in the figure 8, as aircraft approach, the conic cones of the planned tracks will converge in time and space the moment they reach the critical point. The activation condition is when PMR is less than the minimum allowable separation distance (MASD):

$$MASD_{ij} \geq PMR_{ij} \tag{18}$$

$$MASD_{ij} = 2 * DSD + \sum WS_{ij} \tag{19}$$

$$PMR_{\mathrm{ij}} = min\left(\left|P_i\left(t+\Delta t\right) - P_j\left(t+\Delta t\right)\right| - R_i\left(\Delta t\right) - R_j\left(\Delta t\right)\right), \Delta t \subseteq (0, T) \tag{20}$$

$$R\left(\Delta t\right) = 0.425 * \left(\Delta t\right)^2 + 1.19 * \Delta t \tag{21}$$

In figure 8, aircraft A and B are in conflict and aircraft A and C are in conflict. At the current moment, aircraft A and B reach the critical point first, while aircraft A and C do not. Therefore, aircraft A and B activate their strategies simultaneously and maneuver along their planned tracks, while aircraft C continues its normal flight.

IV. EXPERIMENT

In this section, we present a series of simulations to validate the proposed algorithm. Two extreme scenarios are designed for the simulation. One is a five-aircraft scenario and the other is an eight-aircraft scenario. The two scenarios are not common in practice, but extreme scenarios are important and necessary to examine the proposed methodology.

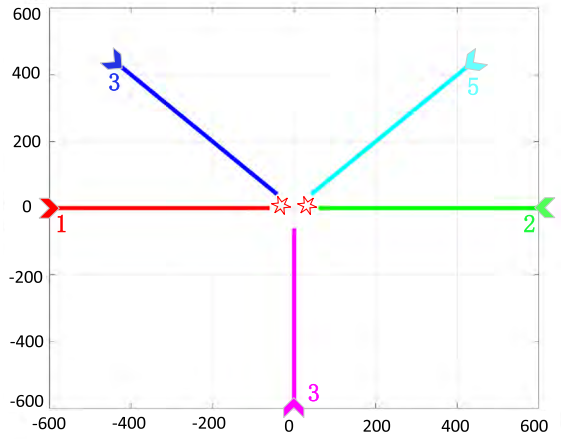

FIGURE 9. The original flight paths of five aircraft.

TABLE 3. Intial state.

Aircraft	Initial position (m, m, m)	Initial speed (m/s)	Initial attitude (rad, rad, rad)
1	(-600, 0, 500)	30	(pi, 0, 0)
2	(600, 0, 500)	30	(pi, 0, 0)
3	(0, -600, 500)	30	(pi/2, 0, 0)
4	$(-300\sqrt{2}, 300\sqrt{2}, 500)$	30	(-pi/4, 0, 0)
5	$300\sqrt{2}, 300\sqrt{2}, 500)$	30	(-3*pi/4, 0, 0)

A. INITIAL CONDITIONS

In this paper, the UAVs are fixed-wing aircraft provided by our team in the College of Aerospace Science and Technology, National University of Defense Technology, China. The mass of each aircraft is 200 kg, the wing span is 8.4 m, the pitch-rate limit is 20 deg/s, and the yaw-rate limit is 20 deg/s. The safe distance is set as 15 m. The safe distance is twice as much as the isolation sphere radius (ISD), ensuring that the isolation spheres of two aircraft will not touch each other. Indeed, the desired separation distance (DSD) is set at 3.1 m, so the ISD is $4.2 + 3.1 = 7.5\ m$, and the safe distance is $7.5 * 2 = 15m$. The safe distance is not fixed and the ISD can be adjusted to satisfy different safety requirements.

B. FIVE-AIRCRAFT SCENARIO

In a local space, five aircraft are cruising at the same speed and at the same altitude. As shown in Figure 9, the tracks of the five aircraft will intersect at the same point and they will meet in a narrow airspace. If no maneuver is taken, a chain collision will occur. Each aircraft will conflict with more than one aircraft. Table 3 records the aircraft's initial states.

Figure 10 shows the entire process in three dimensions. The aircraft maneuver in all directions, including horizontal and vertical, to avoid collisions. At 0 s, the five aircraft start from their initial positions. At 18.0 s, aircraft 4 starts

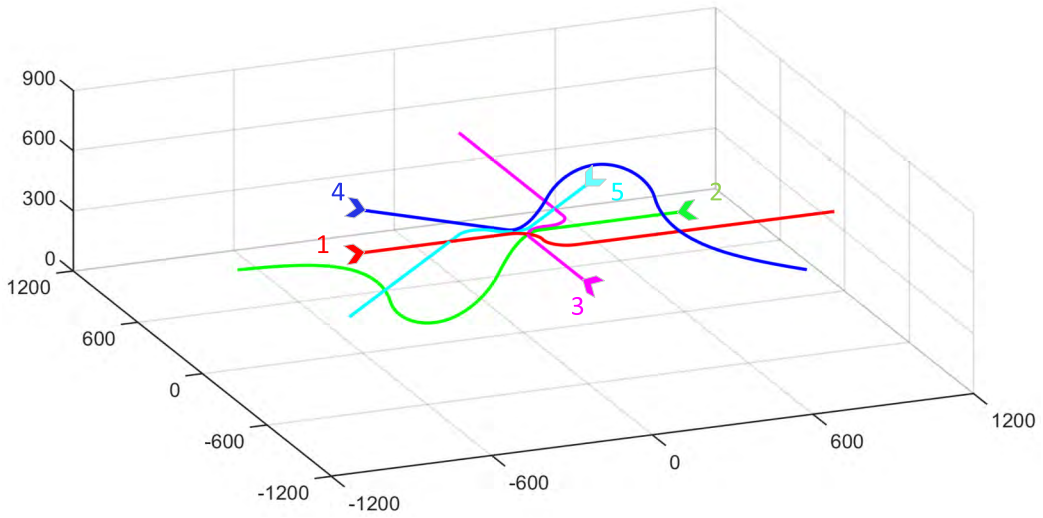

FIGURE 10. The process of collision avoidance in three dimensions.

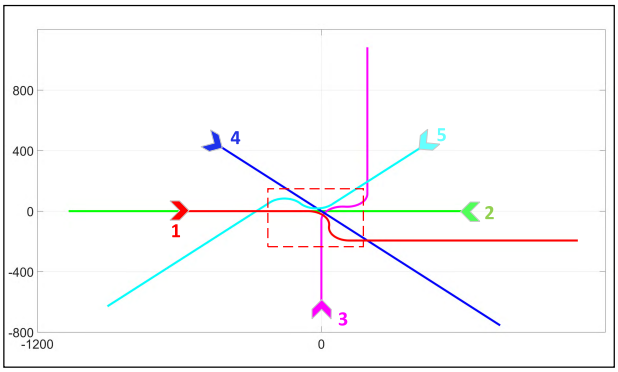

FIGURE 11. The process of collision avoidance on the horizontal plane.

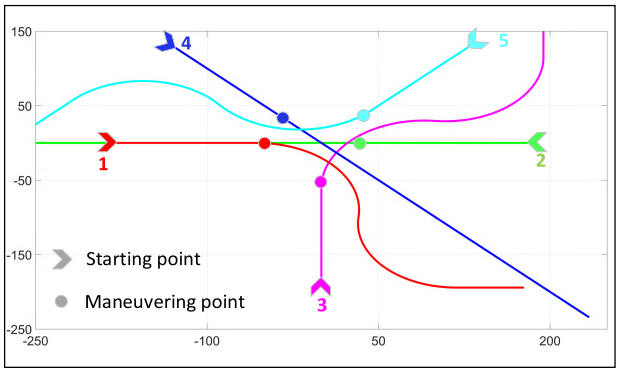

FIGURE 12. The partial process of collision avoidance on the horizontal plane.

climbing with a 1g overload and aircraft 5 rolls slightly to right in a large radius. At 18.1 s, aircraft 2 dives with a -1g overload and aircraft 3 rolls greatly to the left. At 18.2 s, aircraft 1 rolls greatly to the left. In the procedure, each aircraft encounters more than one invader aircraft. Although there is no global resolution, the five aircraft choose their own maneuvers independently and succeed in avoiding a collision by maneuvering once. After maneuvering for five seconds to avoid collisions, the aircraft cross the crowded and threatening area, are not in conflict with other aircraft, and so return to their original tracks.

Figure 11 demonstrates the entire process on the horizontal plane, and Figure 12 demonstrates the local detailed procedure from 13 s to 23 s on the horizontal plane. Aircraft 1, 3, and 5 maneuver in the horizontal direction and aircraft 2 and 4 maneuver in the vertical direction. The activation of this maneuver is about one to three seconds before the collision. The collision-avoidance procedure lasts for five seconds. Thus, the proposed method can simultaneously avoid collisions with aircraft and minimize the interference to the normal aircraft flight as much as possible.

TABLE 4. Minimum distance between pairs.

Aircraft	1	2	3	4	5
1	0	30.6639	24.8899	26.6653	33.0702
2	30.6639	0	22.9592	43.4543	28.0969
3	24.8899	0	0	34.9164	35.3818
4	26.6653	22.9592	34.9176	0	24.7613
5	33.0702	28.0969	35.3818	24.7613	0

Table 4 records the minimum distance between aircraft in the entire procedure. Figure 13 records the Euclidean distance between pairs of aircraft. The minimum distances between pairs are always larger than the safe distance. Thus, the proposed algorithm is valid for the five-aircraft scenario.

C. EIGHT-AIRCRAFT SCENARIO

Eight aircraft in four pairs are in a local space at the same altitude. As shown in Figure 14, the tracks of the eight aircraft will intersect at the same point, and they will meet in a narrow airspace. If no maneuver is taken, a chain collision

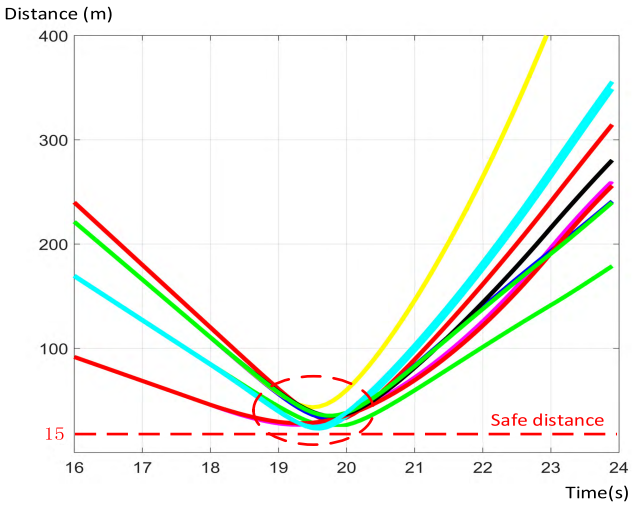

FIGURE 13. The Euclidean distance between pairs of aircraft.

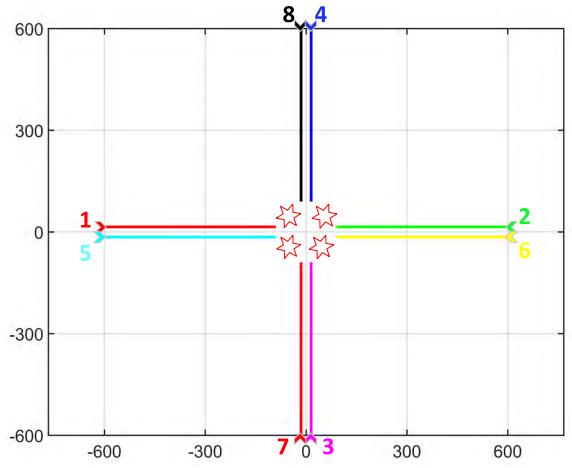

FIGURE 14. The original flight paths of eight aircraft.

TABLE 5. Minimum distance between pairs.

Aircraft	Initial position (m, m, m)	Initial speed (m/s)	Initial attitude (rad, rad, rad)
1	(-600, 10, 500)	30	(0, 0, 0)
2	(600, 10, 500)	30	(pi, 0, 0)
3	(10, -600, 500)	30	(pi/2, 0, 0)
4	(10, 600, 500)	30	(-pi/2, 0, 0)
5	(-600, -10, 500)	30	(0, 0, 0)
6	(600, -10, 500)	30	(pi, 0, 0)
7	(-10, -600, 500)	30	(pi/2, 0, 0)
8	(-10, 600, 500)	30	(-pi/2, 0, 0)

will occur. Each aircraft will conflict with more than one aircraft. Table 5 records the initial aircraft states.

Figure 15 shows the entire process in three dimensions. The aircraft can maneuver in all directions, including horizontal and vertical, to avoid collisions. At 0 s, the eight aircraft in four pairs start from their initial positions. At 17.6 s, aircraft 1 rolls greatly to the left, aircraft 2 rolls greatly to the right, aircraft 3 climbs at a 1g load, aircraft 4 dives at a -1g load, aircraft 5 rolls greatly to the right, aircraft 6 climbs at 1g, aircraft 7 dives at -1g, and aircraft 8 turns greatly to the left. In the procedure, each aircraft encounters more than one invader aircraft. Thus, each aircraft must not only consider the invader aircraft but also its partner in the pair. Although there was no global resolution, the eight aircraft independently chose their own maneuver onboard, and succeeded in avoiding a collision by maneuvering once.

Figure 16 demonstrates the entire process on the horizontal plane, Figure 17 demonstrates the local detailed procedure from 13 s to 23 s on the horizontal plane, and Figure 18

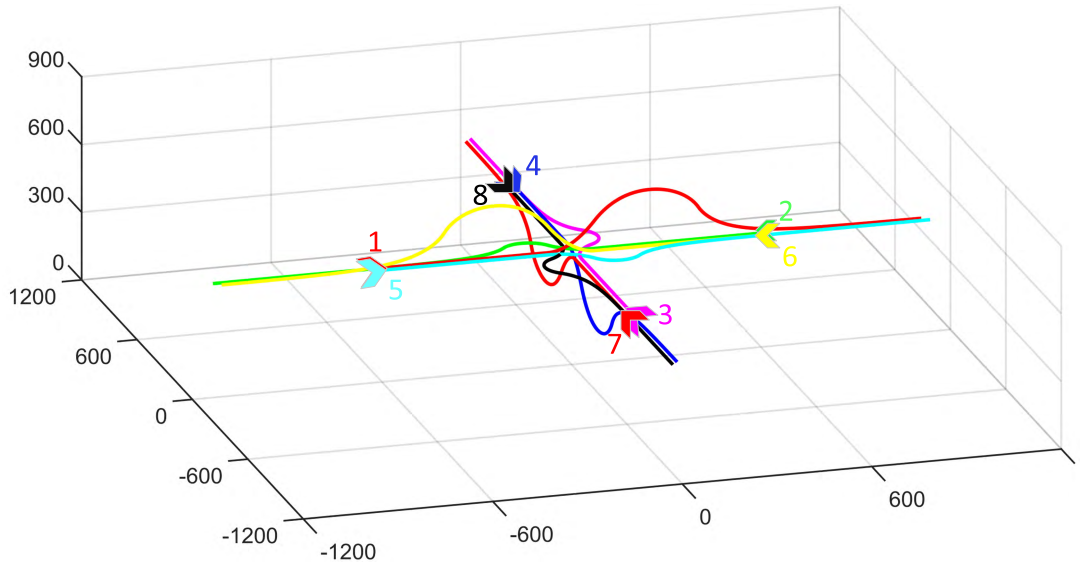

FIGURE 15. The process of collision avoidance in three dimensions.

TABLE 6.

Aircraft	1	2	3	4	5	6	7	8
1	0	33.0271	43.3092	44.9181	20	20	44.9181	19.5920
2	33.0271	0	37.7699	19.5920	53.4147	20	43.3092	37.7699
3	43.3092	37.7699	0	33.0271	37.7699	19.5920	20	53.4147
4	44.9181	19.5920	33.0271	0	43.3092	44.9181	20	20
5	20	53.4147	37.7699	43.3092	0	33.0271	19.5920	37.7699
6	20	20	19.5920	44.9181	33.0271	0	44.9181	43.3092
7	44.9181	43.3092	20	20	19.5920	44.9181	0	33.0271
8	19.5920	37.7699	53.4147	20	37.7699	43.3092	33.0271	0

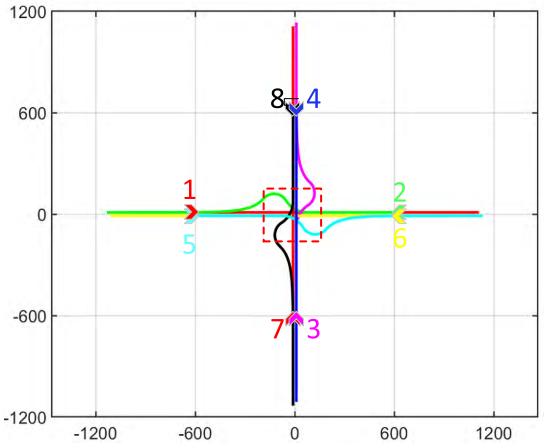

FIGURE 16. The process of collision avoidance on the horizontal plane.

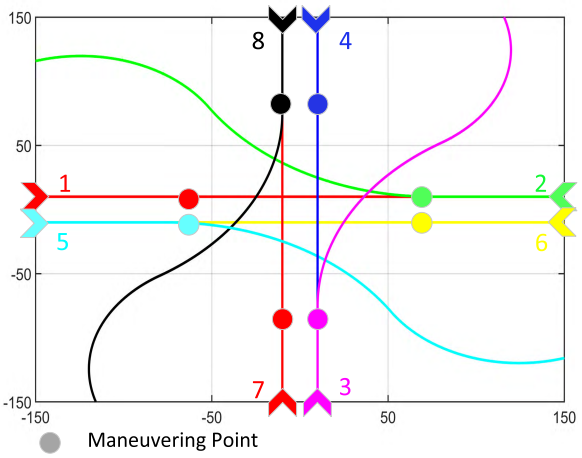

FIGURE 17. The partial process of collision avoidance on the horizontal plane.

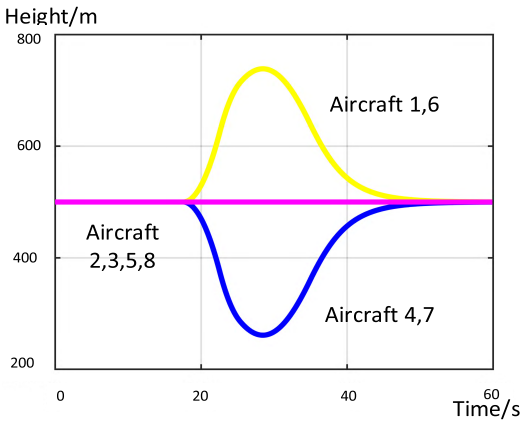

FIGURE 18. The partial process of collision avoidance on the vertical plane.

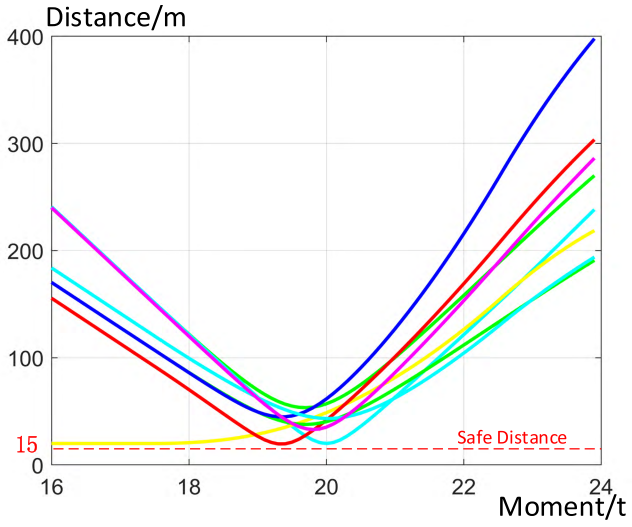

FIGURE 19. The Euclidean distance between pairs of aircraft.

demonstrates the process on the vertical plane. Aircraft 2, 3, 5, and 8 maneuver in the horizontal direction, and aircraft 1, 4, 6, and 7 maneuver in the vertical direction. The activation of the maneuver is about one to three seconds before the collision. After five seconds of CA, the eight aircraft succeed in crossing the crowded and dangerous zone; however, their original formations are broken. After maneuvering, at 22.6 s, the aircraft begin to return to their original tracks and restore their original formations.

Table 6 records the minimum distance between aircraft in the entire procedure. Figure 19 records the Euclidean distance between aircraft pairs. The minimum distances between pairs are larger than the safe distance. The proposed methodology is valid for the eight-aircraft scenario. It simultaneously avoided aircraft collision and minimized the interference to the normal flight of aircraft as much as possible.

V. CONCLUSION

In this paper, a novel distributed CDR algorithm was proposed for multiple UAVs. The algorithm performed an

automatic, aggressive CD strategy. Each aircraft chose three candidate strategies from a pre-set pool of strategies and generated corresponding planned tracks. Then, it coordinated with other aircraft in the network and determined the primary strategy. When a collision was about to occur, the CA maneuver was activated.

The following conclusions were drawn:

(1) The study's main contribution was proposing a distributed CDR algorithm for multiple UAVs, based on key-node selection and strategy coordination. The proposed CDR algorithm effectively processed conflicts between multiple aircraft in a highly dynamic, high-density environment.

(2) This paper proposed a novel CD algorithm that integrated the spatial and temporal dimensions. It overcame the great defect of traditional CD algorithms and is suitable for aircraft formations and clusters.

(3) This paper introduced uncertainty modeling in aircraft track prediction. A cone was formed by combining the trajectory generated by six-degrees-of-freedom motion with an error radius. The uncertainty modeling improved the robustness of the system and greatly eliminated the uncertainty.

(4) This paper introduced a special token-allocation method, which solved the problem of coordination with incomplete information and partial environmental knowledge.

Recommendations and future work are as follows: (1) Further improve the method's operational efficiency and meet the need for faster-than-real-time on a single processor. (2) Further validate the method in complex situations, especially with clusters of aircraft and continuous conflicts.

REFERENCES

[1] Y. Morsly, N. Aouf, and M. S. Djouadi, "Dynamic decentralized/centralized free conflict UAV's team allocation," in *Proc. IEEE Int. Instrum. Meas. Technol. Conf.*, May 2012, pp. 2340–2345.

[2] M. Alighanbari and J. How, "Robust decentralized task assignment for cooperative UAVs," in *Proc. AIAA Guid., Navigat., Control Conf. Exhibit*, vol. 1, 2006, p. 6454.

[3] J. Tang and W. Yang, "A causal model for safety assessment purposes in opening the low-altitude urban airspace of chinese pilot cities," *J. Adv. Transp.*, vol. 2018, Oct. 2018, Art. no. 5042961.

[4] J.-W. Park, H.-D. Oh, and M.-J. Tahk, "UAV collision avoidance based on geometric approach," in *Proc. SICE Annu. Conf.*, vol. 1, Aug. 2008, pp. 2122–2126.

[5] S.-C. Han, H. Bang, and C.-S. Yoo, "Proportional navigation-based collision avoidance for UAVs," *Int. J. Control, Automat. Syst.*, vol. 7, no. 4, pp. 553–565, 2009.

[6] J. Goss, R. Rajvanshi, and K. Subbarao, "Aircraft conflict detection and resolution using mixed geometric and collision cone approaches," in *Proc. AIAA Guid., Navigat., Control Conf. Exhibit*, 2004, p. 4879.

[7] C. Carbone, U. Ciniglio, F. Corraro, and S. Luongo, "A novel 3D geometric algorithm for aircraft autonomous collision avoidance," in *Proc. 45th IEEE Conf. Decis. Control*, vol. 1, no. 1, Dec. 2006, pp. 1580–1585.

[8] S. Luongo, F. Corraro, U. Ciniglio, V. Di Vito, and A. Moccia, "A novel 3D analytical algorithm for autonomous collision avoidance considering cylindrical safety bubble," in *Proc. IEEE Aerosp. Conf.*, Mar. 2010, pp. 1–13.

[9] A. L. Smith and F. G. Harmon, "UAS collision avoidance algorithm based on an aggregate collision cone approach," *J. Aerosp. Eng.*, vol. 24, no. 4, pp. 463–477, 2010.

[10] Y. Wan, J. Tang, and S. Lao, "Research on the collision avoidance algorithm for fixed-wing UAVs based on maneuver coordination and planned trajectories prediction," *Appl. Sci.*, vol. 9, no. 4, p. 798, 2019.

[11] K. Sigurd and J. How, "UAV trajectory design using total field collision avoidance," in *Proc. AIAA Guid., Navigat., Control Conf. Exhibit*, vol. 1, 2003, p. 5728.

[12] J. Y. Liu, Z. Q. Guo, and S. Y. Liu, "The simulation of the UAV collision avoidance based on the artificial potential field method," *Adv. Mater. Res.*, vol. 591, pp. 1400–1404, Nov. 2012.

[13] S. Temizer, M. Kochenderfer, L. Kaelbling, T. Lozano-Pérez, and J. Kuchar, "Collision avoidance for unmanned aircraft using Markov decision processes," in *Proc. AIAA Guid., Navigat., Control Conf.*, 2010, p. 8040.

[14] P. E. Hart, N. J. Nilsson, and B. Raphael, "A formal basis for the heuristic determination of minimum cost paths," *IEEE Trans. Syst. Sci. Cybern.*, vol. 4, no. 2, pp. 100–107, Jul. 1968.

[15] J.-M. Alliot, N. Durand, and G. Granger, "FACES: A free flight autonomous and coordinated embarked solver," *Air Traffic Control Quart.*, vol. 8, no. 2, pp. 109–130, 2000.

[16] A. Richards and J. P. How, "Aircraft trajectory planning with collision avoidance using mixed integer linear programming," in *Proc. Amer. Control Conf.*, vol. 3, May 2002, pp. 1936–1941

[17] J. van den Berg, S. J. Guy, M. Lin, and D. Manocha, "Reciprocal *n*-body collision avoidance," in *Robotics Researc*. Springer, 2011, pp. 3–19.

[18] J. Holt, S. Biaz, and C. A. Aji, "Comparison of unmanned aerial system collision avoidance algorithms in a simulated environment," *J. Guid., Control, Dyn.*, vol. 36, no. 3, pp. 881–883, 2013.

[19] P. Brooker, "STCA, TCAS, airproxes and collision risk," *J. Navigat.*, vol. 58, no. 3, pp. 389–404, 2005.

[20] A. Gotlieb, "TCAS software verification using constraint programming," *Knowl. Eng. Rev.*, vol. 27, no. 3, pp. 343–360, 2012.

[21] T. B. Wolf and M. J. Kochenderfer, "Aircraft collision avoidance using Monte Carlo real-time belief space search," *J. Intell. Robot. Syst.*, vol. 64, no. 2, pp. 277–298, Nov. 2011.

[22] T. Jun, M. A. Piera, and S. Ruiz, "A causal model to explore the ACAS induced collisions," *Proc. Inst. Mech. Eng., G, J. Aerosp. Eng.*, vol. 228, no. 10, pp. 1735–1748, 2014.

[23] M. A. Skoog, "Automatic air collision avoidance system (Auto-ACAS)," Nat. Aeronaut. Space Admin. Edwards AFB CA Dryden Flight, Tech. Rep., 2003.

[24] R. Turner *et al.*, "Automatic aircraft collision avoidance algorithm design for fighter aircraft," in *Proc. Asia-Pacific Int. Symp. Aerosp. Technol.*, 2012.

[25] J. Wadley *et al.*, "Development of an automatic aircraft collision avoidance system for fighter aircraft," in *Proc. AIAA Infotech. Aerosp. Conf. (IA)*, vol. 1, 2013, p. 4727.

[26] J. Roskam, *Airplane Flight Dynamics and Automatic Flight Controls*. Lawrence, KS, USA: DARcorporation, 1998.

[27] G. Granger, N. Durand, and J.-M. Alliot, "Token allocation strategy for free-flight conflict solving," in *Proc. 13th Innov. Appl. Artif. Intell. Conf.*, 2001, pp. 59–64.

YU WAN received the bachelor's degree from the National University of Defense Technology (NUDT), Changsha, China, in 2017, where he is currently pursuing the M.S. degree. During his B.S. study, he focused on system engineering and operation research. After that, he focused on theories and methods of collision avoidance of aircraft. His research interests include the air traffic management and unmanned aerial vehicle systems, such as collision avoidance of aircraft.

JUN TANG was dedicated to the Ph.D. research with the Technical Innovation Cluster on Aeronautical Management, Universitat Autònoma de Barcelona (UAB). He is currently an Assistant Professor with the Science and Technology on Information Systems Engineering Laboratory, National University of Defense Technology. He acted as one of the main participants playing an important role in the FP7 European project Innovative Technologies and Researches for a New Airport Concept towards Turnaround Coordination (INTERACTION) with collaboration of Airbus. His research interests include logistic systems, causal modeling, state space, air traffic management, and discrete event simulation (DES). He was the Winner of the William Sweet Smith Prize, in 2015. He is very active in the simulation community and organizing as a General Co-Chair of several international conferences.

SONGYANG LAO received the B.S. degree in information system engineering and the Ph.D. degree in system engineering from the National University of Defense Technology, Changsha, China, in 1990 and 1996, respectively. In 1996, he joined the National University of Defense Technology, as a Faculty Member. From 2004 to 2005, he was a Visiting Scholar with Dublin City University. He is currently a Professor with the School of Information System and Management, National University of Defense Technology. His current research interests include image processing and video analysis, and human–computer interaction.